Random Matrix Theories for Dirac Operators at finite Lattice Spacing

STONY BROOK UNIVERSITY

M. Kieburg, J.J.M. Verbaarschot, and S. Zafeiropoulos

Unterstützt von / Supported by Alexander von Humboldt Stiftung / Foundation

and by U.S. DOE Grant No. DE-FG-88ER40388

Introduction

In the low energy limit, QCD exhibits universal behavior that agrees with Random Matrix Theory (RMT) reflecting the symmetries of the Dirac operator. In the continuum limit as well as for finite lattice spacing $a \neq 0$ we have constructed random matrix ensembles with the eigenvalue correlations of QCD.

The models under consideration consist of matrices D_a whose entries are weighted by independent Gaussian distributions. In the continuum limit, with lattice spacing $a = 0$, and quark mass $m = 0$, the chiral Gaussian Unitary Ensemble (chGUE) is defined by:

$$D_0 = \begin{bmatrix} 0 & W \\ -W^\dagger & 0 \end{bmatrix} \quad \text{, weighted by} \quad P(D_0) \propto \exp(-n\mathrm{tr}\, WW^\dagger)\,, \tag{1}$$

where W is a $n \times (n+\nu)$ complex matrix and ν is the topological charge. **The matrix dimension plays the role of the lattice volume, i.e.** $n \sim V$. The matrix D_0 reflects the chiral symmetry of the Dirac-operator in the continuum limit, i.e. $\gamma_5 D_0 = -D_0\gamma_5$ with $\gamma_5 = (\mathbb{1}_n, -\mathbb{1}_{n+\nu})$ [1]. For the eigenvalue density of this random matrix theory in the quenched case,

$$\rho(z) \propto \int d[D_0]P(D_0)\mathrm{tr}\,\delta(z - D_0), \tag{2}$$

we find in the microscopic limit

$$\rho\left(\frac{\imath x}{2n}\right) \overset{n\gg1}{=} \nu\delta(x) + \frac{\sqrt{\pi n}}{2}|x|\left[J_\nu^2(x) - J_{\nu-1}(x)J_{\nu+1}(x)\right] \tag{3}$$

with $x \in \mathbb{R}$ and J_l are Bessel functions of the first kind. This result also follows from the microscopic limit of the chiral Lagrangian for the Dirac spectrum. The Dirac-distribution corresponds to the ν generic zero eigenvalues.

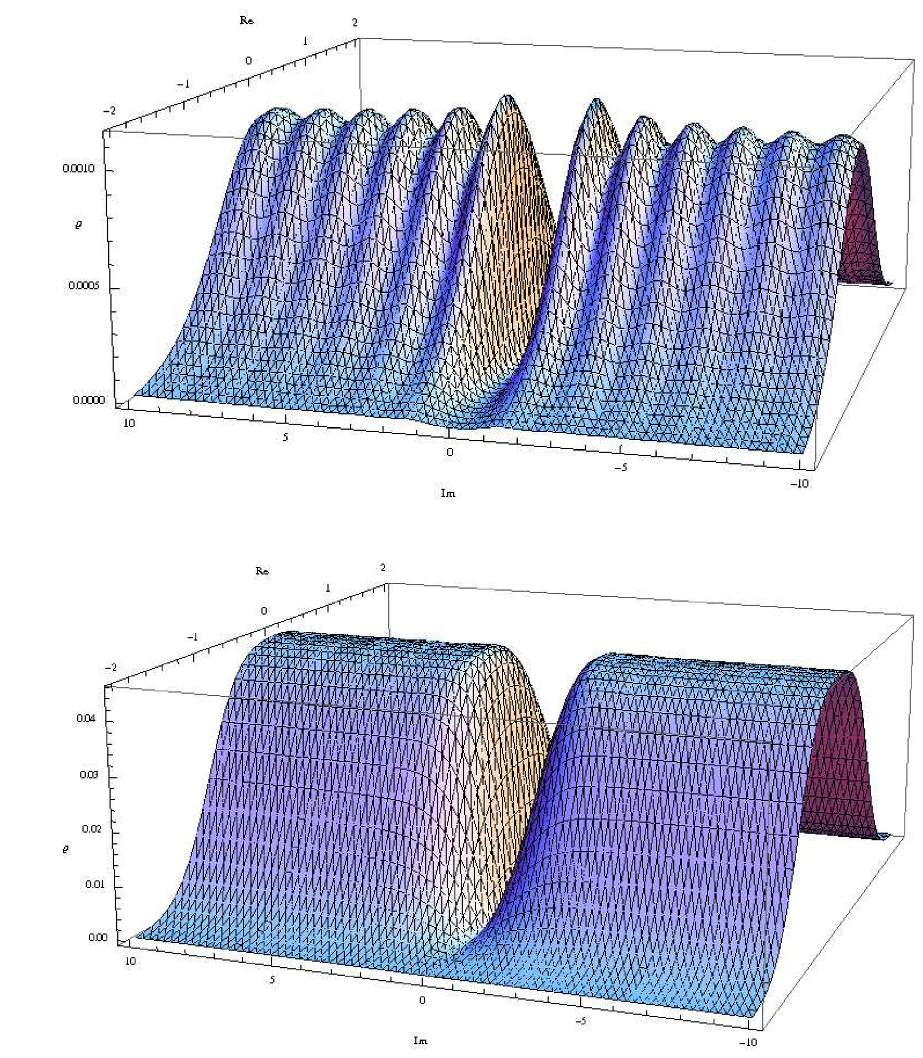

Fig. 1: Both figures show the analytical results for the eigenvalue distribution ρ_c with topological charge $\nu = 1$. The upper figure is for the rescaled lattice spacing $\hat a = 0.2$ and the lower one for $\hat a = 2$. The imaginary axis is scaled by $1/n$ whereas the real axis has the scale $\hat a^2/n$. The distribution ρ_c is given in arbitrary units. The oscillations of continuum QCD vanishes for large $\hat a$.

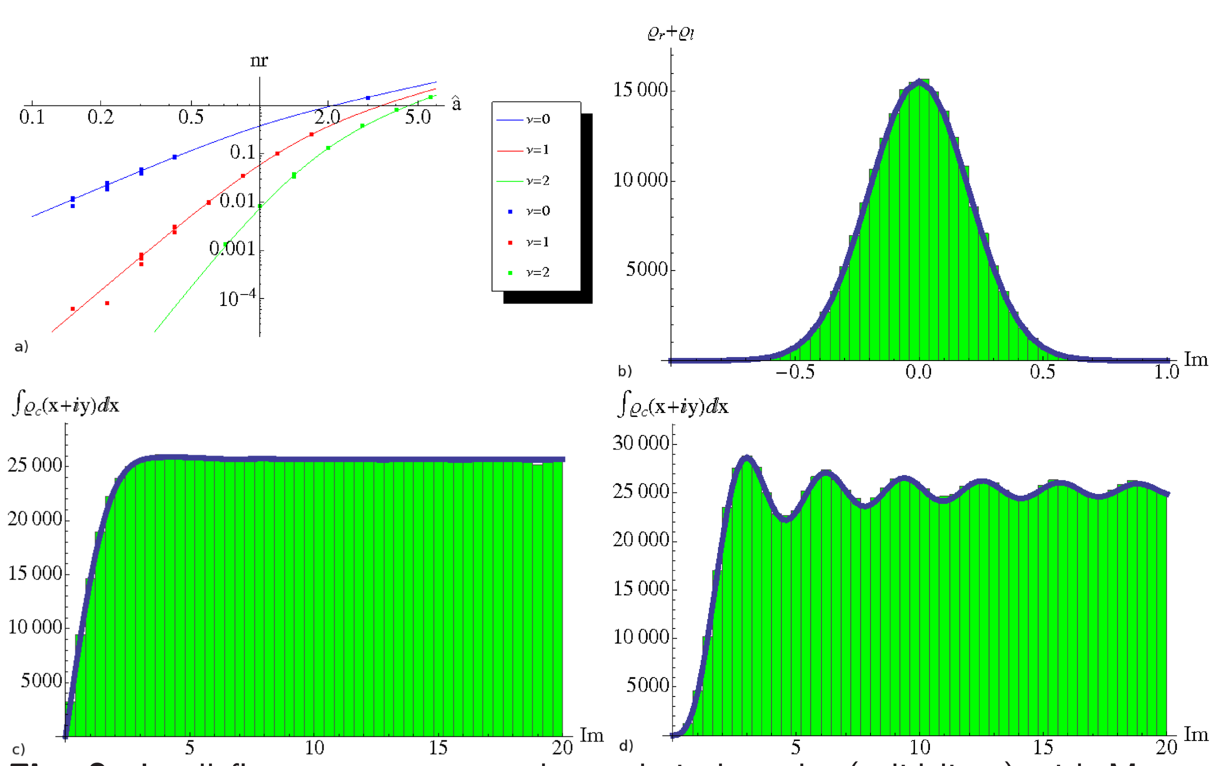

Fig. 2: In all figures we compare the analytical results (solid lines) with Monte Carlo simulations (points or histograms). The additional real eigenvalues for $\hat a$ and for various ν are shown in figure a). The matrix size as well as the number of matrices vary in this plot. In the log-log plot b) we draw the distribution of real eigenvalues for $\nu = 1$ and $\hat a = \sqrt{2}/10$. Figures c) and d) display the projection of the distribution ρ_c on the imaginary axis for ($\nu = 0, \hat a = \sqrt{2}$) and ($\nu = 1, \hat a = \sqrt{2}/10$), respectively. We performed the Monte Carlo simulations in b), c) and d) for ensembles of 200000 matrices and $n = 50$.

All figures are in perfect agreement with the numerical simulations. They reveal that the critical value for the dimensionless lattice spacing $\hat a$ is around 1. If it is larger than 1 the structures of continuum QCD are smoothened out.

The evd of the Wilson-Dirac Operator

For the Wilson-Dirac operator we consider the RMT

$$D_W = \begin{bmatrix} A & W \\ -W^\dagger & B \end{bmatrix} \quad \text{, weighted by} \quad P(D_W) \propto \exp\left[-\frac{n}{2a^2}(\mathrm{tr}\, A^2 + \mathrm{tr}\, B^2) - n\mathrm{tr}\, WW^\dagger\right], \tag{4}$$

where the $n \times n$ Hermitian matrix A and the $(n+\nu)\times(n+\nu)$ Hermitian matrix B break the chiral symmetry [2-4]. **In the large n limit we fix $2na^2 = \hat a^2$ as a constant which is consistent with the ϵ counting scheme of Wilson chiral perturbation theory.** We have derived analytical expressions for the eigenvalue density (evd) of the complex eigenvalues, ρ_c, and of the real eigenvalues, separately for the right- and left-handed eigenvectors, ρ_r and ρ_l. The densities ρ_r and ρ_l are related by

$$\rho_l(x) = \rho_r(x) + \rho_{\mathrm{GUE}}^{(\nu)}(x) + \rho_{\mathrm{int}}(x) = \rho_r(x) + \rho_\chi(x)\,, \tag{5}$$

where ρ_χ is the chirality distribution. The distribution $\rho_{\mathrm{GUE}}^{(\nu)}$ is the evd of the Gaussian unitary ensemble of dimension ν. The interaction term ρ_{int} represents the repulsion between the ν generic real eigenvalues with the remaining ones and, thus, is not a distribution, i.e. not positive definite. The term ρ_{int} vanishes for $\hat a \to 0$. For $n \gg 1$ we find

$$\rho_c\left(\frac{z}{2n}\right) \propto \frac{\sqrt{n}}{\hat a}|y|\int \exp\left[-\hat a^2\left(\left[\cos\varphi_1 - \frac{x}{2\hat a^2}\right]^2 + \left[\cos\varphi_2 - \frac{x}{2\hat a^2}\right]^2\right)\right]\sin^2\left(\frac{\varphi_1-\varphi_2}{2}\right)\mathrm{sinc}[y(\cos\varphi_1-\cos\varphi_2)]\cos[\nu(\varphi_1+\varphi_2)]d\varphi_1 d\varphi_2\,, \tag{6}$$

$$\rho_r\left(\frac{x}{2n}\right) \propto \int \frac{\sin^2[(\varphi_1-\varphi_2)/2]\cos[\nu(\varphi_1+\varphi_2)]}{\cos\varphi_1-\cos\varphi_2}\left[\exp\left[\delta_1^2-\delta_2^2\right]\mathrm{erf}\left[\delta_1,\sqrt{2}\delta_1\right] - \exp\left[\delta_2^2-\delta_1^2\right]\mathrm{erf}\left[\delta_2,\sqrt{2}\delta_2\right]\right]d\varphi_1 d\varphi_2\,,\ \delta_j = \hat a\left(\cos\varphi_j - \frac{x}{2\hat a^2}\right)\,, \tag{7}$$

$$\rho_\chi\left(\frac{x}{2n}\right) \propto \frac{1}{\hat a^2}\int \frac{\exp\left[-([s_1-x]^2+[s_2+\imath x]^2)/(4\hat a^2)\right]}{s_1 - \imath s_2} s_1^\nu\left[s_1K_{\nu+1}(s_1)I_\nu(\imath s_2) + \imath s_2 K_\nu(s_1)I_{\nu+1}(\imath s_2)\right]\delta^{(\nu-1)}(s_1)ds_1 ds_2 \tag{8}$$

with $z = x + \imath y$ and $x, y \in \mathbb{R}$. The functions erf, I_l, K_l and $\delta^{(l)}$ are the generalized incomplete error function, the modified Bessel function of the first and second kind and the l-th derivative of the Dirac distribution, respectively. The normalization is chosen as

$$\int \rho_c\left(\frac{z}{2n}\right)d[z] = 2n\,,\quad \int \rho_\chi\left(\frac{x}{2n}\right)dx = \nu\,,\quad \int \rho_r\left(\frac{x}{2n}\right)dx \propto \hat a^{2(\nu+1)} \tag{9}$$

for small lattice spacing. These results are shown and compared to Monte Carlo simulations in Figs. 1 and 2.

The evd of the Dirac Operator for Staggered Fermions

We study a random matrix ensemble for the staggered Dirac operator that captures its main discretization effects. The model is defined by

$$D_{st} = \begin{bmatrix} 0 & 0 & W + a\widetilde W & aC \\ 0 & 0 & aB & W^\top - a\widetilde W^\top \\ -W^\dagger - a\widetilde W^\dagger & -aB^\dagger & 0 & 0 \\ -aC^\dagger & -W^* + a\widetilde W^* & 0 & 0 \end{bmatrix}\text{, weighted by}\quad P(D_{st}) \propto \exp\left[-n\left(\mathrm{tr}\, WW^\dagger + \mathrm{tr}\,\widetilde W\widetilde W^\dagger + \frac{\mathrm{tr}\, CC^\dagger}{2} + \frac{\mathrm{tr}\, BB^\dagger}{2}\right)\right], \tag{10}$$

where W, $\widetilde W$ are $n\times(n+\nu)$ and B, C are $(n+\nu)\times(n+\nu)$ and $n\times n$ complex matrices, respectively. It is a simplified version of the random matrix theory proposed in [5,6]. For $a = 0$, this model has $2^{\lfloor d/2\rfloor}$ flavors for d dimensions with ν zero modes for each flavor, while at $a \neq 0$ we have flavor mixing and zero modes are absent. The spectral density exhibits two chGUE's for $a \ll 1/\sqrt{n}$ and becomes one chGUE when $a \gg 1/\sqrt{n}$. The spectral flow with a shows avoided level crossings when lattice artifacts start dominating the Dirac spectrum. Monte Carlo simulations are shown in Fig. 3.

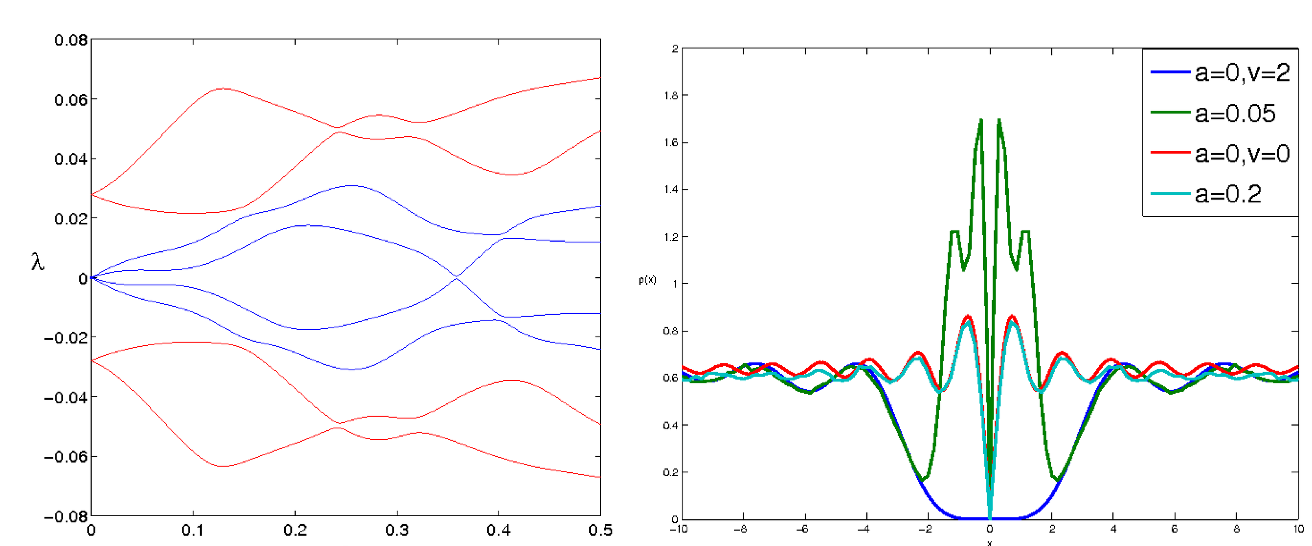

Fig. 3: The left figure shows the typical spectral flow of staggered eigenvalues for $\nu = 2$ and the right figure gives the quenched spectral density of D_{st} for various values of ν and the non-rescaled lattice spacing a. The results for the spectral density are generated by Monte Carlo simulations for an ensemble of 100000 matrices with $n = 50$.

Conclusions

- **Wilson-Dirac Operator:** For $\hat a < 1$: $\nu = 0$ gives most of the additional real eigenvalues. It behaves as $\hat a^2$ whereas the number of real eigenvalues for $\nu \neq 0$ is suppressed by higher orders in $\hat a$.
- **Staggered Fermions:** The scale $1/\sqrt{n}$ (i.e. $1/\sqrt{V}$ in lattice QCD) determines the appearance of lattice artifacts with increasing $\hat a$.

References

[1] E.V. Shuryak and J.J.M. Verbaarschot, Nucl. Phys. A 560:306-320, 1993.

[2] S.R. Sharpe and R.L. Singleton, Phys. Rev. D 58:074501, 1998.

[3] P.H. Damgaard, K. Splittorff, and J.J.M. Verbaarschot, Phys. Rev. Lett. 105:162002, 2010.

[4] G. Akemann, P.H. Damgaard, K. Splittorff, and J.J.M. Verbaarschot, Phys. Rev. D 83:085014, 2011.

[5] J.C. Osborn, Nucl. Phys. Proc. Suppl. 129:886-888, 2004.

[6] J.C. Osborn, Phys. Rev. D 83:034505, 2011.